Journal of Molecular Catalysis A: Chemical 358 (2012) 49–57

Contents lists available at SciVerse ScienceDirect

Journal of Molecular Catalysis A: Chemical

journal homepage: www.elsevier.com/locate/molcata

Physico-chemical properties of lutetium phthalocyanine complexes in solution and in solid polystyrene polymer fibers and their application in photoconversion of 4-nitrophenol

Ruphino Zugle, Tebello Nyokong*

Department of Chemistry, Rhodes University, Grahamstown 6140, South Africa

ARTICLE INFO

Article history:
Received 27 December 2011
Received in revised form 3 February 2012
Accepted 20 February 2012
Available online 27 February 2012

Keywords:
Lutetium phthalocyanine
Phenoxy
Pyridiloxy
Electrospinning
Nitrophenol
Photocatalysis

ABSTRACT

The photophysical and photochemical behavior of two phthalocyanine complexes of lutetium peripherally substituted with tetraphenoxy and tetra-2-pyridiloxy groups were studied in solution and when dispersed in polystyrene polymer fiber. The phthalocyanines were found not to fluoresce significantly in solution and not at all within the fiber matrix as compared with standard unsubstituted zinc phthalocyanine. They showed very promising photoactivity in solution with high singlet oxygen quantum yields. Their photoactivity within the polymer fiber matrix was also demonstrated with the photoconversion of 4-nitrophenol, a water pollutant. The photodegradation process with both phthalocyanines follows first order kinetics similar to that observed for the zinc phthalocyanine and the photo-products were found to be hydroquinone, benzoquinone and 4-nitrocatechol.

1. Introduction

Phthalocyanines have been employed in various technological applications such as in photo-conversion of pollutants [1], read-write compact discs [2], non-linear optics [3] and photodynamic therapy [4]. This is due to the fact that their properties can be fine-tuned in many ways through changes in the type of coordinating metal [5,6] as well as structural changes in the phthalocyanine ligand moiety [7]. Alkoxy and alkyl substituents for example, are known to enhance the solubility of the phthalocyanines in common solvents thus rendering them easier to be applied in homogeneous systems [8,9]. The presence of axial coordinating ligands is also known to influence the physico-chemical properties of these phthalocayanines [10].

Phthalocyanines may be employed as catalysts either in solution or in their solid state as well as when dispersed in solid support systems [2,9,11]. For phthalocyanines in the solid state or on solid support systems, the theory of molecular exciton is usually used to rationalize the differences between the optical spectra in the liquid phase and those in the solid state [12–14]. Also equally important is the fact that the photophysical and photochemical properties of the phthalocyanines can be altered when on supports since they are constrained within the environment of a polymeric matrix and therefore their behavior within the resulting material cannot be directly extrapolated from the known behavior in a solution [13].

This study is therefore aimed at the spectroscopic and physico-chemical behavior of novel peripherally substituted phthalocyanine complexes of lutetium; 2,(3), 9(10), 16(17), 23(24)-(tetraphenoxyphthalocyaninato) lutetium(III) acetate (**3a**) and 2,(3), 9(10), 16(17), 23(24)-(tetra-2-pyridiloxyphthalocyaninato) lutetium(III) acetate (**3b**), Scheme 1, both in solution and in a solid polystyrene fiber matrix. We further assessed the photoactivity of the phthalocyanine containing polymer fibers for the photodegradation of 4-nitrophenol and compared these with a similar polymer fibers containing standard unsubstituted zinc phthalocyanine. Pyridiloxy and phenoxy substituents for the phthalocyanines have been well researched for many central metals and metalloids [15–17]. The choice of lutetium in this work was influenced by its larger size which will encourage intersystem crossing to the triplet state, hence generating singlet oxygen which is required for photocatalysis. Also the applications of the lanthanide phthalocyanines in photocatalysis are still rare in the literature. The synthesis and photophysical behavior of lutetium phthalocyanine substituted at non-peripheral position with phenoxy groups have been reported [17], in the current work phenoxy groups are on the peripheral position. The effects of the pyridiloxy versus phenoxy substituents on the phthalocyanine on their photochemical behavior within the fiber matrix will be investigated.

* Corresponding author. Tel.: +27 46 6038260; fax: +27 46 6225109.
E-mail address: t.nyokong@ru.ac.za (T. Nyokong).

1381-1169/$ – see front matter © 2012 Elsevier B.V. All rights reserved.
doi:10.1016/j.molcata.2012.02.010

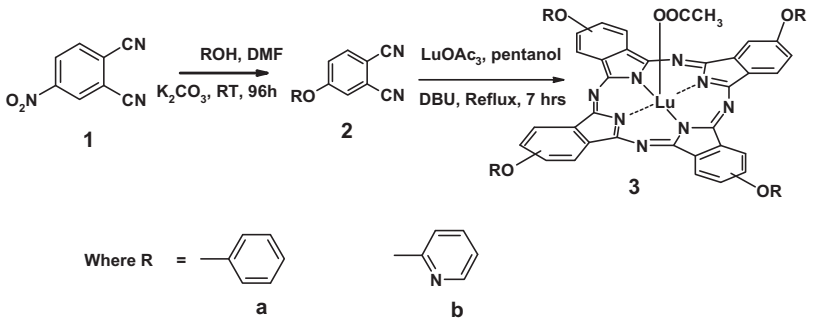

Scheme 1. Synthetic scheme for **3a** and **3b**.

2. Experimental

2.1. Materials

The following chemicals were purchased from SAARCHEM; *n*-hexane, dimethylsulfoxide (DMSO), N,N-dimethylfomamide (DMF), tetrahydofuran (THF) and dichloromethane (DCM). Zinc phthalocyanine (ZnPc), 1,8-diazabicyclo[5.4.0] undec-7-ene (DBU), 1,3-diphenylisobenzofuran (DPBF), lutetium(III) acetate, deuterated dimethylsulfoxide (DMSO-d_6), anthracene-9,10-bis-methylmalonate (ADMA), benzoquinone, 4-nitrocatechol and polystyrene (PS) were from Sigma Aldrich and hydroquinone from May and Baker. Ultra-pure water (Milli-Q water system, Millipore Corp., Bedford, MA, USA) was used for all photocatalyzed sample solutions. Phosphate buffer solutions were prepared using reagent grade potassium dihydrogen orthophosphate (ACE) and dipotassium phosphate (PAL chemicals). 4-Nitrophthalonitrile (**1**) was synthesized according to literature procedures [18]. Compounds **2a** and **2b** were prepared through base catalyzed nucleophilic aromatic displacement reaction as described in the literature [15,19,20].

Column chromatography was performed on silica gel 60 (0.04–0.063 mm) and preparative thin layer chromatography on silica gel 60 P F_{254}.

2.2. Equipment

Infrared (IR) spectra were recorded on a Perkin-Elmer Fourier transform – IR (100 FT-IR) spectrophotometer. UV–vis absorption spectra were recorded on a Shimadzu UV-2550 spectrophotometer. ^{1}H NMR spectra were recorded on a Bruker AMX600 MHz in detuerated DMSO. Microanalyses were performed using a Vario-Elementar Microcube ELIII. Mass spectral data were recorded on ABI Vogager De-STR Maldi TOF instrument using α-cyano-4-hydroxycinnamic acid as a matrix. Scanning electron microscope (SEM) images were obtained using a JOEL JSM 840 scanning electron microscope.

Irradiations for singlet oxygen studies were done using General Electric Quartz lamp (300 W), 600 nm glass (Schott) and water filters, to filter off ultra-violet and far infrared radiations respectively. An interference filter 670 nm with bandwidth of 40 nm was placed in the light path just before cell containing the sample.

Bruker Vertex 70-Ram II Raman spectrometer (equipped with a 1064 nm Nd:YAG laser and a liquid nitrogen cooled germanium detector) were used to collect Raman data. The Raman spectral data for **3a**/PS, **3b**/PS and PS were obtained from the electrospun fibers.

Fluorescence excitation and emission spectra were recorded on a Varian Cary Eclipse spectrofluorimeter. Fluorescence lifetimes were measured using a time correlated single photon counting setup (TCSPC) (Fluo Time 200, Picoquant GMbH) with a diode laser as excitation source (LDH-P-670 driven by PDL 800-B, 670 nm, 20 MHz repetition rate, Picoquant GmbH). Fluorescence was detected under the magic angle with a peltier cooled photomultiplier tube (PMT) (PMA-C 192-N-M, Picoquant GmbH) and integrated electronics (PicoHarp 300E, Picoquant GmbH). A monochromator with a spectral width of about 4 nm was used to select the required emission wavelength. The response function of the system, which was measured with a scattering Ludox solution (DuPont), had a full width at half-maximum (FWHM) of about 300 ns. The ratio of stop to start pulses was kept low (below 0.05) to ensure good statistics. All luminescence decay curves were measured at the maximum of emission peak. The data were analyzed with the program FluoFit (Picoquant GmbH). The support plane approach [21] was used to estimate the errors of the decay times.

Fluorescence images of the fibers were taken with a DMLS fluorescence microscope. The excitation source was a high-voltage mercury lamp and light in the wavelength range of 550–730 nm.

2.3. Photophysical and photochemical parameters

2.3.1. Triplet state yields and lifetimes

Triplet quantum yields were determined for **3a** and **3b** in DMF using a comparative method [22], Eq. (1), with ZnPc as a standard.

$$\Phi_T = \Phi_T^{Std} \frac{\Delta A_T \varepsilon_T^{Std}}{\Delta A_T^{Std} \varepsilon_T} \quad (1)$$

where ΔA_T and ΔA_T^{Std} are the changes in the triplet state absorbances of the samples (**3a** and **3b**) and the standard, respectively. ε_T and ε_T^{Std} are the triplet state molar extinction coefficients for the samples (**3a** and **3b**) and the standard, respectively. Φ_T^{Std} is the triplet quantum yield for the standard, ZnPc ($\Phi_T^{Std} = 0.58$ in DMF) [23]. The triplet lifetimes were determined by exponential fitting of the kinetic curves using the program ORIGIN Pro 8.

2.3.2. Fluorescence quantum yields

Fluorescence quantum yields (Φ_F) of the phthalocyanines were determined in DMF by the comparative method [24], Eq. (2)

$$\Phi_F = \Phi_F^{Std} \frac{FA_{Std} n^2}{F_{Std} A n_{Std}^2} \quad (2)$$

where F and F_{Std} are the areas under the fluorescence emission curves of samples (**3a** and **3b**) and the standard, respectively. A and A_{Std} are the respective absorbances of the samples and standard at the excitation wavelength. The same solvent was used for samples and standard. Unsubstituted ZnPc in DMF ($\Phi_F^{Std} = 0.30$) [25] was employed as the standard. Both the samples and standard were excited at the same wavelength of 633 nm and emission spectrum was recorded from 650 nm to 790 nm. The absorbances of the solutions at the excitation wavelength were about 0.05 to avoid any inner filter effects.

2.3.3. Singlet oxygen quantum yields

A chemical method was also employed to determine the singlet oxygen quantum yields, Φ_Δ, of **3a** and **3b** in DMF. The comparative method was used with ZnPc ($\Phi_\Delta^{ZnPc} = 0.56$ in DMF) [26–28], as standard and DPBF as singlet oxygen quencher.

The relative method shown by Eq. (3), was employed in calculating Φ_Δ.

$$\Phi_\Delta = \Phi_\Delta^{ZnPc} \cdot \frac{R^{Sample} \cdot I^{ZbPc}}{R^{ZnPc} \cdot I^{Sample}} \quad (3)$$

where Φ_Δ^{ZnPc} is the singlet oxygen quantum yield for the ZnPc standard, R^{sample} and R^{ZnPc} are the DPBF photobleaching rates in the presence of compound **3a** or **3b** and ZnPc standard respectively, while I^{sample} and I^{ZnPc} are the respective rates of light absorption by compound **3a** or **3b** and ZnPc standard. The initial DPBF concentrations were kept the same for both the standard and the sample. Molar extinction coefficient ($dm^3\ mol^{-1}\ cm^{-1}$) of DPBF at $\lambda = 417$ nm in DMF $\varepsilon = 23{,}000$ [29].

For the modified fibers (**3a**/PS, **3b**/PS and ZnPc/PS), the singlet oxygen quantum yield (Φ_Δ) determinations were carried out in aqueous solutions using ADMA as the quencher and its degradation was monitored at 380 nm. In each case 10 mg of the modified fibers was suspended (as small pieces) in an aqueous solution of ADMA and similarly irradiated using the photolysis set-up described above. The quantum yields (Φ_{ADMA}) were estimated using Eq. (4), using the extinction coefficient of AMDA in water $\log(\varepsilon) = 4.1$ [30].

$$\Phi_{ADMA} = \frac{(C_0 - C_t)V_R}{I_{abs} \cdot t} \quad (4)$$

where C_0 and C_t are the ADMA concentrations prior to and after irradiation, respectively; V_R is the solution volume; t is the irradiation time per cycle and I_{abs} is defined by Eq. (5).

$$I_{abs} = \frac{\alpha \cdot A \cdot I}{N_A} \quad (5)$$

where $\alpha = 1\text{–}10^{-A(\lambda)}$, $A(\lambda)$ is the absorbance of the sensitizer at the irradiation wavelength, A is the irradiated area (2.5 cm^2), I is the intensity of light (4.54×10^{16} photons $cm^{-2}\ s^{-1}$) and N_A is Avogadro's constant.

The absorbances used for Eq. (5) are those of the phthalocyanines in the fibers (not in solution) measured by placing the modified fiber directly on a glass plate. The light intensity measured refers to the light reaching the spectrophotometer cells, and it is expected that some of the light may be scattered, hence the Φ_Δ values of the phthalocyanines in the fiber are estimates. The singlet oxygen quantum yields Φ_Δ were calculated using Eq. (6) [31]

$$\frac{1}{\Phi_{ADMA}} = \frac{1}{\Phi_\Delta} + \frac{1}{\Phi_\Delta} \cdot \frac{k_d}{k_a} \cdot \frac{1}{[ADMA]} \quad (6)$$

where k_d is the decay constant of singlet oxygen in the respective solvent and k_a is the rate constant of the reaction of ADMA with $O_2(^1\Delta_g)$. The intercept obtained from the plot of $1/\Phi_{ADMA}$ versus 1/[ADMA] gives $1/\Phi_\Delta$.

2.4. Photocatalytic reactions

Photocatalytic reactions were carried out in a magnetically stirred batch reactor (glass vial). The irradiation experiments were carried out using the photolysis set-up described above for singlet oxygen detection. The intensity of the light reaching the reaction vessel was measured with a power meter (POWER MAX 5100, Molelectron Detector Inc.) and found to be 3.52×10^{20} photons $cm^{-2}\ s^{-1}$. The transformation was monitored by observing the absorption band (400 nm) of 4-nitrophenol after each photolysis cycle of fifteen minutes using a Shimadzu UV-2550 spectrophotometer. The experiments were carried out using a variety of concentrations of 4-nitrophenol in pH 8.2 phosphate buffer. Each sample solution (4 mL) contained 20 mg of functionalized fiber.

2.5. Chromatographic analysis

The photolysis products were separated and analyzed using both gas chromatography (GC) and by direct injection into ion trap mass spectrometer fitted with an electrospray ionization (ESI-MS) mass spectra. For gas chromatographic analyses, an Agilent Technologies 6820 GC system fitted with a DB-MS Agilent J & W GC column was employed. A Finnigan MAT LCQ ion trap mass spectrometer equipped with an electro-spray ionization (ESI) source was used for mass analysis. Spectra were acquired in the negative ion mode, with the capillary temperature set at 200 °C and sheath gas set at 60 arbitrary units, with the capillary and tube lens voltage set at −20 and −5 V respectively. The aqueous photocatalyzed sample solution was extracted with dichloromethane and then injected into the GC.

2.6. Synthesis

*2.6.1. Synthesis of 2,(3), 9(10), 16(17), 23(24)-(tetraphenoxyphthalocyaninato) lutetium(III) acetate (**3a**), Scheme 1*

A mixture of anhydrous lutetium(III) acetate (134 mg, 0.38 mmol), 4-phenoxyphthalonitrile (**2a**) (339 mg, 1.54 mmol) in 1-pentanol (2 mL) was refluxed for 7 h under nitrogen atmosphere with DBU as catalyst. After cooling, the crude product was precipitated with *n*-hexane, filtered and washed with excess *n*-hexane and then air dried. Column chromatography (silica gel) was employed using THF: methanol (10:1) as the eluting solvent mixture. Yield: 25%. IR [KBr, υ cm^{-1}] 773, 824, 883, 938, 1039, 1067 (Pc skeleton), 1224, 1264, 1390, 1467, 1482 (C—O—C), 1606, 1714, 1770 (C=O), 2927, 2957 (C—H, aromatic), 3058 (CH_3). UV–vis (DMF): λ_{max} nm ($\log\varepsilon$) 351 (4.51) 610 (5.11), 678 (5.78). Calcd. for $C_{58}H_{35}N_8O_6Lu$; C 62.48%, H 3.16%, N 10.05%. Found C 62.00%, H 3.32%, N 10.24%; ^{1}H NMR (DMSO-d): δ, ppm 7.79–7.91 (12-H, m, Pc-H), 6.88–6.97 (20-H, m, Phenyl-H), 1.99 (3-H, s, acetate-CH_3); (ES^+), (m/z): Calc. 1115; Found: 1116 [M+H$^+$].

*2.6.2. Synthesis of 2,(3), 9(10), 16(17), 23(24)-(tetra-2-pyridiloxyphthalocyaninato) lutetium(III) acetate (**3b**), Scheme 1*

The synthesis of **3b** was as outlined for **3a** except **2b** instead of **2a** was employed. The amounts of the reagents were the same as well as the purification procedures. Yield: 23%. IR [KBr, υ cm^{-1}] 837, 910, 1012, 1057, 1077, 1133 (Pc skeleton), 1269, 1355, 1384, 1489 (C—O—C), 1654, 1719, 1769 (C=O), 2927, 2957 (C—H, aromatic), 3053 (CH_3). UV–vis (DMF): λ_{max} nm ($\log\varepsilon$) 337 (4.74) 613 (5.26), 678 (5.94). Calcd. for $C_{54}H_{31}N_{12}O_6Lu$; C 57.97%, H 2.79%, N 15.02%. Found C 58.14%, H 3.01%, N 14.89%; ^{1}H NMR (DMSO-d): δ, ppm 7.76–8.67 (12-H, m, Pc-H), 6.78–7.27 (16-H, m, Pyridyl-H), 2.11 (3-H, s, acetate-CH_3); (ES^+), (m/z): Calc. 1119; Found: 1120 [M+H$^+$].

2.6.3. Preparation of functionalized fibers

The fibers were prepared using the electrospinning method reported before [32] with modifications as follows: a solution containing 2.5 g (1.3×10^{-5} moles) of polystyrene (PS) and 1.35 mg each of compound **3a**, **3b** or ZnPc, in 10 ml DMF/THF(4:1) was stirred for 24 h to produce a homogeneous solution. The solvent mixture was employed to allow both PS and the phthalocyanines to dissolve. The solution was then placed in a cylindrical glass tube fitted with a capillary needle. A potential difference of 20 kV was applied to provide charge for the spinning process. The distance

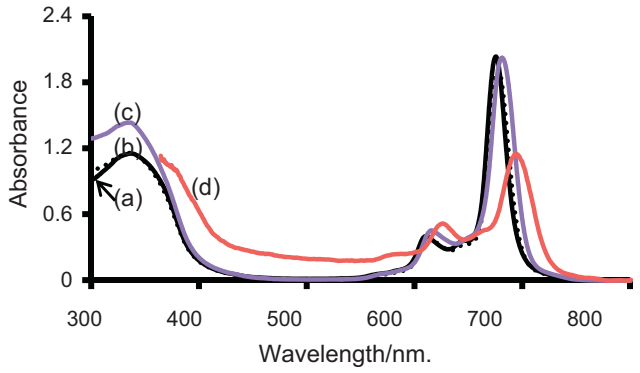

Fig. 1. UV–vis spectra of compound **3b** in (a) THF, (b) DMF, (c) DMSO and (d) on PS fiber. Solution concentration ~2.0×10^{-6} M.

between the cathode (static fiber collection point) and anode (tip of capillary needle) was 15 cm and pump rate was 0.01 mL/h. The flow rate was however increased to 0.02 mL/h in the case of the polystyrene/phthalocyanine composite to avoid sputtering of the solution. ZnPc/PS fibers were similarly prepared.

3. Results and discussion

3.1. Spectral and microscopic characterization

The electronic absorption spectra of compound **3b** (as a representative of both complexes) in THF, DMF and DMSO are shown in Fig. 1. Narrow Q bands were observed in solution suggesting monomeric in nature of the complexes [33,34]. As shown, there is a slight red shift in the Q band absorption as the solvent is changed from THF to DMSO. This is explained in terms of the coordinating tendency of the solvents [35]. A similar trend was observed for compound **3a** as shown in Table 1.

There is more red-shifting in the Q band in moving from solution to the solid state polymer fiber matrix. The red shift in the Q-band of the phthalocyanines within the fiber core compared to solutions could be attributed to the electronic interaction between the Pc and the polymer resulting in lower energy states. Such a bathochromic shift in the electronic spectral features of photosensitizers as a result of interactions with other molecules has been reported for porphyrins [36] and phthalocyanines [37]. The strong π–π interaction due to the stacking of the rings leads to broadening of the Q band as observed in Fig. 1d. The observation of a Q band in the fiber confirms successful incorporation of the complexes into the fiber matrix.

Raman spectra were employed to further confirm the presence of the Pc in the fiber. The peaks between 2500 and 3000 cm^{-1} (Fig. 2a) in the Raman spectrum of the PS alone are attributed to

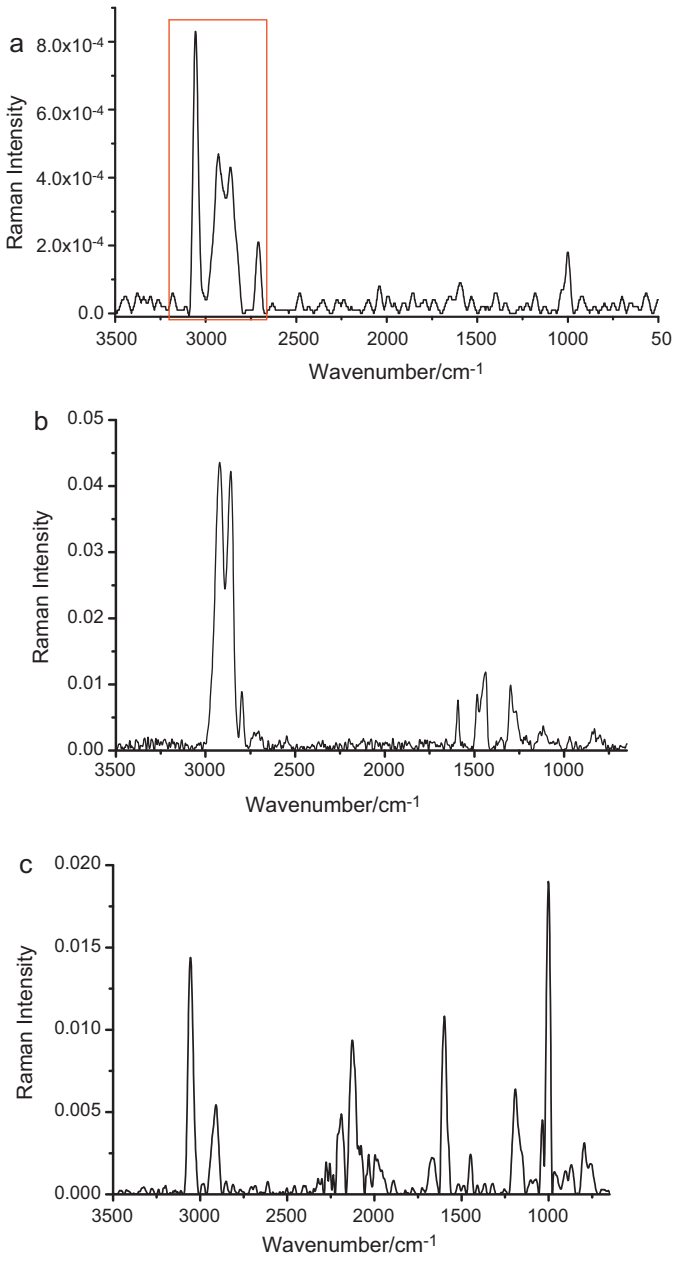

Fig. 2. Raman spectra of (a) PS fiber, (b) **3a**/PS composite fiber and (c) **3b**/PS composite fiber.

Table 1
Spectroscopic and photophysical data for complexes **3a** and **3b**.

Parameter	Solvent	3a	3b
λ_Q (nm)	THF	676	675
	DMF	678	677
	DMSO	683	681
	Fiber	693	693
Φ_F	DMF	<0.01	0.017
Φ_T	DMF	0.71	0.68
Φ_Δ [a]	DMF	0.68 (0.28)	0.62 (0.17)
τ_T (μs)	DMF	2.60 ± 0.01	2.64 ± 0.01
τ_{F1} (ns)[b]	DMF	4.27 ± 0.31 (0.09)	4.60 ± 0.21 (0.14)
τ_{F2} (μs)[b]	DMF	0.10 ± 0.04 (0.91)	0.11 ± 0.04 (0.86)

[a] Values in brackets are for complexes **3a** and **3b** in fiber matrix. Φ_Δ for ZnPc in DMF = 0.56 [26], Φ_Δ for ZnPc/PS in aqueous solution = 0.13.
[b] Relative amplitudes shown in brackets.

stretches due to the aromatic ring [38]. Any electronic interaction between the polystyrene and the phthalocyanines is mostly likely to involve the π-electrons of their aromatic systems. The bands corresponding to the aromatic regions in the composite fibers (Fig. 2b and c) have increased intensities compared to the polymer fiber alone. Most importantly, the observed changes in the peak positions and/or splitting of the PS fiber bands in the composites suggest that the phthalocyanines are interacting very strongly with the polystyrene aromatic system.

The fiber morphology and diameters were assessed using scanning electron microscopy. Both **3a**/PS and **3b**/PS and PS fibers alone did not form appreciable amount of beads and consist of mostly long unbranched strands of cylindrical fibers as shown in Fig. 3.

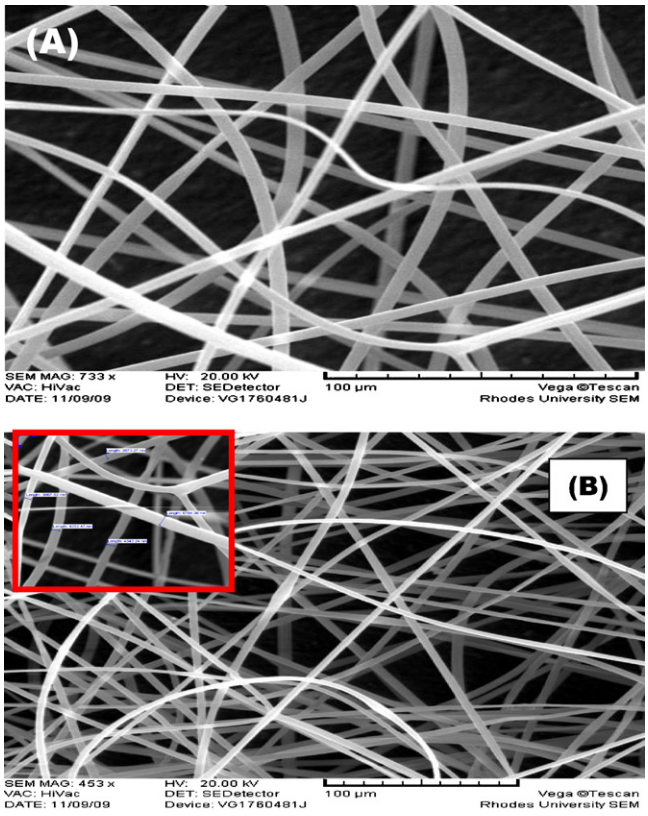

Fig. 3. Fiber mat of (a) polystyrene alone and (b) **3a**/polystyrene composite at 100 μm resolution and insert is 50 μm resolution.

3.2. Photophysical and photochemical properties

3.2.1. Triplet quantum yield and lifetimes

Singlet oxygen which is mostly implicated in photosensitized reactions is produced through transfer of energy from the excited triplet state of the photosensitizer to ground state molecular oxygen [39]. Thus the ability of a sensitizer to undergo the spin forbidden transition from its excited singlet state to the triplet state is a fundamental requirement for photosensitization processes. In this work, we determined the fraction of the excited singlet state molecules of **3a** and **3b** that can undergo the intersystem crossing to the triplet state (triplet quantum yield, Φ_T) by using Eq. (1).

Fig. 4a shows the triplet state decay profiles for compound **3a** as a representative. Monoexponential decay kinetics were obeyed. The lifetimes for the triplet states were found to be 2.60 ± 0.01 μs and 2.64 ± 0.01 μs in DMF for **3a** and **3b** respectively (Table 1). The triplet lifetimes are lower than is typical of Pcs due to the large size of the Lu central metal. Triplet quantum yields were found to be 0.71 and 0.68 for **3a** and **3b** respectively (Table 1). Pyridiloxy substituent on **3b** is electron donating and electron donors are known [40] to quench excited triplet states hence the slightly lower value of Φ_T for **3b**.

3.2.2. Fluorescence spectra, quantum yields and lifetimes

The fluorescence properties of **3a** and **3b** were examined in spectroscopic grade DMF degassed with argon. The fluorescence spectra for **3a** and **3b** were mirror images of the excitation spectra, Fig. 5 (**3b** is representative of both **3a** and **3b**). As observed in Fig. 5, the Q-band maxima of the absorption and excitation spectra in both cases are in close proximity. This suggests that the nuclear configuration of the ground states and excited states are similar and not

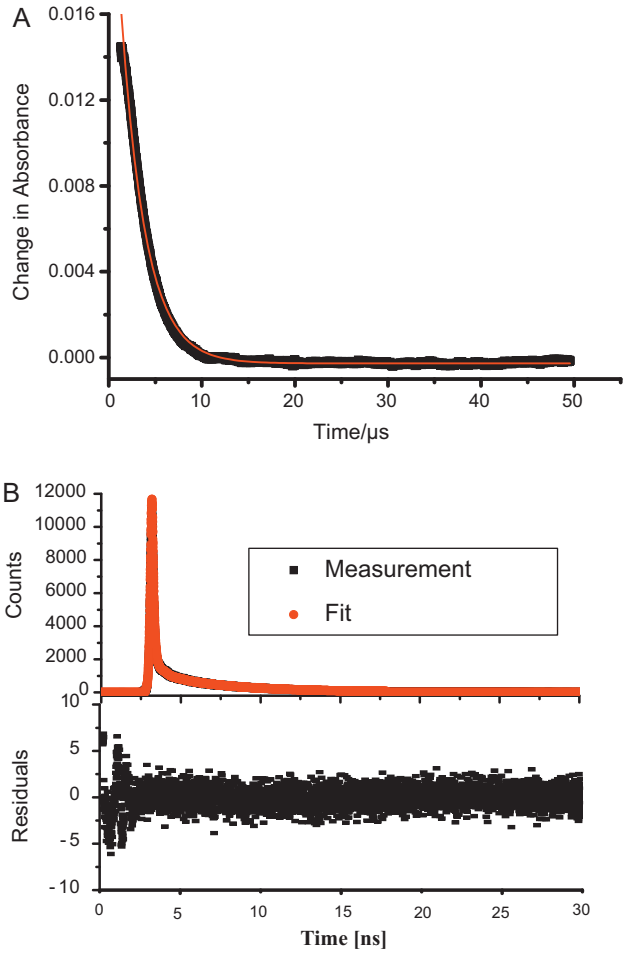

Fig. 4. Triplet decay curve at 490 nm (a) and fluorescence decay profile (b) for compound **3a** in DMF. Excitation wavelength 673 nm for triplet yield studies. For TCSPC trace excitation was at the maximum of the emission peak at 695 nm.

affected by excitation in the solvent. The stokes shifts are typical of metallophthalocyanine complexes [41].

The fluorescence quantum yields (Φ_F) were determined in DMF, using a comparative method. The values obtained were <0.01 and 0.017 for **3a** and **3b**, respectively, Table 1. The low Φ_F values obtained could be attributed to the heavy atom effect of the central lutetium coordinating diamagnetic atom which encourages intersystem crossing to its excited triplet state leading to high triplet quantum yields observed in this work. A similar argument has also been suggested for hafnium phthalocyanines which do not

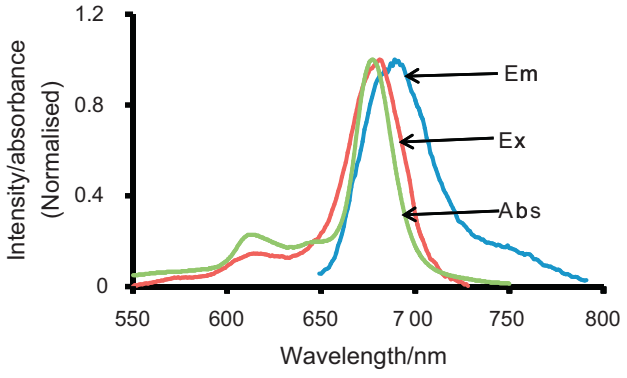

Fig. 5. Fluorescence (Em), absorption (Abs), excitation (Ex) spectra in DMF for **3b**.

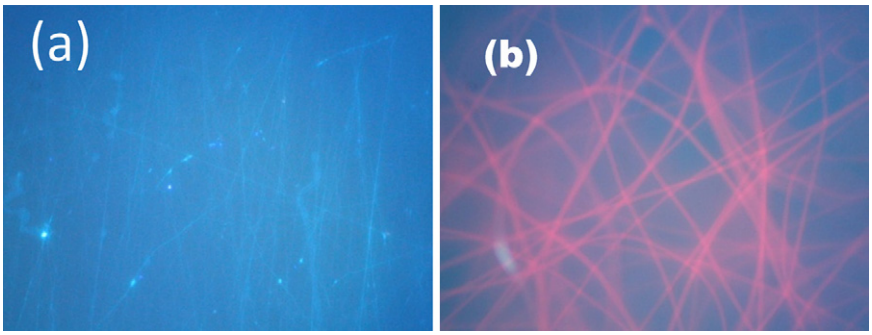

Fig. 6. Fluorescence micrographs of PS fibers functionalized with (a) compound **3a** and (b) ZnPc.

fluoresce at all [42]. The slightly higher Φ_F for **3b** corresponds to the lower Φ_T.

The fluorescence decay of the phthalocyanines, Fig. 4b for **3a** (representing both complexes) show biexponential fluorescence decay profile. The lifetimes and amplitudes are listed in Table 1. Biexponential fluorescence decay profiles of phthalocyanines are attributed to the formation of ground-state dimers which can quench the monomer fluorescence leading to a quenched and unquenched lifetimes [43]. In this work two lifetimes were observed for both **3a** and **3b**.

The fluorescence behavior of **3a** and **3b** in the functionalized fiber were assessed by taking fluorescence micrographs by exciting the functionalized fibers with a high-voltage mercury lamp using a filter in the wavelength range of 550–730 nm. Both functionalized fibers did not show the characteristic fluorescence as compared with similar polystyrene polymer fibers functionalized with the known fluorescent unsubstituted zinc phthalocyanine (ZnPc) as shown in Fig. 6. This could be due to their low fluorescence observed in solution and coupled with the stacking of their molecules in the solid state which usually make phthalocyanine molecules non-emissive [44].

3.2.3. Singlet oxygen quantum yield

There are a number of unrelated factors that determine the magnitude of singlet oxygen yield for any photosensitizer. These include the energy of excited triplet state of the sensitizer, the extent to which substituents on the phthalocyanine and the solvent medium can quench the singlet oxygen as well as the lifetime of the excited triplet state and the efficiency of the energy transfer between the excited triplet state of the sensitizer and the ground state molecular oxygen. In our case, compounds **3a** and **3b** have comparable triplet state quantum yield. The singlet oxygen yields for **3a** and **3b** were found to 0.68 and 0.62 respectively. This relatively higher singlet oxygen quantum of compound **3a** in DMF over that of **3b** can only be attributed to their differences in Φ_T values and their efficiencies in energy transfer from the triplet state to ground state oxygen.

The singlet oxygen quantum yields of the **3a** and **3b** within the polymeric fibers were determined in water since the fibers will be applied for the transformation of 4-nitrophenol in aqueous media. ADMA was used as singlet oxygen quencher in aqueous media. Fig. 7 shows the degradation profile of ADMA in solutions containing **3a**/PS fibers in water upon irradiation. Similar spectral changes were observed for the **3b**/PS or ZnPc/PS fibers. The Pcs did not leach out of solution as observed in Fig. 7 since they are bound within the fiber matrix and are also not water soluble. No degradation of ADMA was observed under similar conditions when PS fiber was used without functionalization with phthalocyanines. The singlet oxygen quantum yields were 0.28, 0.17 and 0.13 for **3a**/PS, **3b**/PS and ZnPc/PS, respectively. These values are significantly lower than those obtained when the Pcs were in DMF solution and can be explained in two contexts. First, it could be due to the fact that the photophysical and photochemical behavior of the phthalocyanine can be altered when constrained within the environment of a solid polymeric matrix. Thus a direct correlation between the phthalocyanine behavior in solution and in solid fiber matrix cannot be feasible. Such an assertion has been put forward by Lang et al. [13]. Secondly, equally important is the fact that such lowering of the singlet oxygen quantum yield of phthalocyanines in protic solvents such as water has been observed [45]. It is believed that such a decrease is due to interaction between the vibrational levels of the solvent molecules and the electronic or vibrational levels of singlet oxygen resulting in deactivation of the singlet oxygen in such solvents. Also as stated above the Φ_Δ values for Pcs in fibers are an estimate.

Nonetheless, the singlet oxygen quantum yields suggest that functionalized fibers are promising photosensitizers that could be applied in the photo-conversion of various analytes. Thus we applied the fabric materials for conversion of 4-nitrophenol.

3.2.4. Photoconversion of 4-nitrophenol

We further established that the functionalities of the phthalocyanines are maintained within the fiber matrices by using the functionalized fibers for the conversion of 4-nitrophenol in the presence of visible light.

Nitroaromatic compounds are recognized as environmentally hazardous [46]. Nitrophenols in particular are classified as priority pollutants by United State Environmental Protection Agency. Due to their poisonous nature, various remediation processes from the environmental media have been suggested [47–50].

The use of energy from the electromagnetic spectrum is cost effective and remains much more practical approach to the conversion of these pollutants to less toxic products. Phthalocyanines in particular are very promising sensitizers for such photocatalytic applications. Their maximum light absorption occurs in the visible portion of the electromagnetic spectrum, which constitutes a

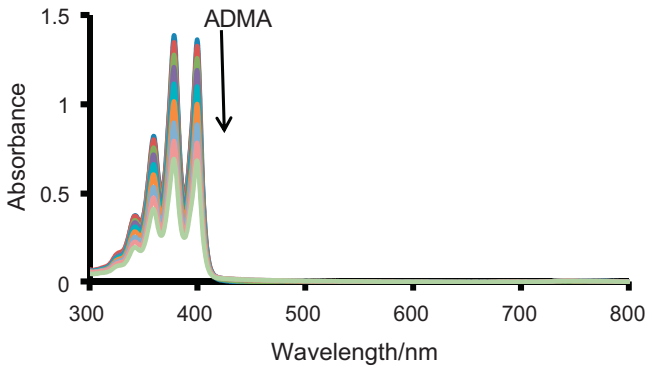

Fig. 7. UV–vis spectral changes observed on photolysis of ADMA in water with **3a**/PS fiber as sensitizer. Spectra taken at 15 min intervals.

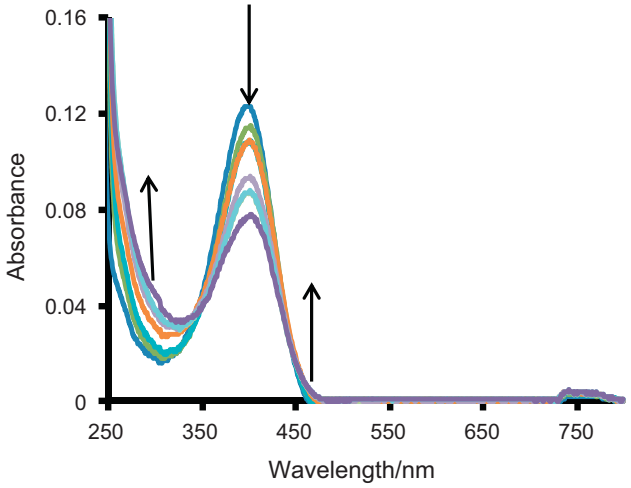

Fig. 8. Electronic absorption spectral changes of observed during photolysis of 4-Np using 20 mg polystyrene fiber functionalized with compound **3a** in pH 8.2 buffer solution.

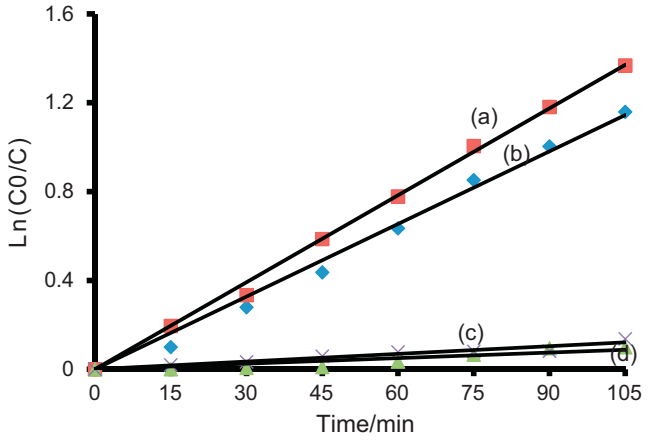

Fig. 9. Effect of addition of singlet oxygen quencher (sodium azide) on the transformation rate of 2.5×10^{-4} M 4-Np in air using (a) **3a**/PS fiber without sodium azide, (b) **3b**/PS fiber without sodium azide, (c) **3a**/PS fiber with sodium azide and (d) **3b**/PS fiber with sodium azide. 20 mg of **3a** or **3a** used in all cases.

larger portion of the spectrum and thus more available than the ultra-violet portion required by other sensitizers [51,52].

In this work we use 4-nitrophenol as a representative nitrophenol. The photocatalytic reaction was carried out in a buffer aqueous solution of pH 8.2 which is slightly higher than the pK_a 7.15 of 4-nitrophenol [53]. It is known that the deprotonated forms of substituted phenols are much more easily oxidizable by singlet oxygen [54]. Fig. 8 shows the UV–vis spectral changes of 4-nitrophenol solution during the photolysis process. As shown, the peak around 400 nm that corresponds to 4-nitrophenol decreases in intensity with irradiation in the presence of the functionalized fiber. There are corresponding increases in the absorbance around 280 and 455 nm, suggesting the formation of photodegradative products of 4-nitrophenol. Similar spectral observations were made with the polystyrene fiber functionalized with compound **3b**, though the changes were slightly less pronounced. This could possibly be due to higher singlet oxygen quantum yield of compound **3a** than **3b** in the fiber as determined in aqueous media. However, when non functionalized polystyrene polymer fiber was used under similar conditions, no spectral changes of the aqueous 4-nitrophenol sample solutions was observed. This suggests that the phthalocyanines (**3a** and **3b**) are the agents involved in the phototransformation process due to their ability to generate the reactive singlet oxygen. Similarly, when only the 4-nitrophenol sample solution was irradiated with the visible light no spectral changes were observed further suggesting that the catalysis can only occur in the presence of the sensitizer.

We assessed the supposed involvement of singlet oxygen in the conversion of 4-nitrophenol by conducting the photolysis reaction with and without sodium azide, a singlet oxygen quencher, in the sample solutions. Fig. 9 shows the kinetics of the various reaction conditions using first order kinetic model. There is generally a good fit with R^2 values above 0.96 in all cases. As shown in Fig. 9, the phototransformation reaction is slowed when sodium azide is added to 4-nitrophenol solution. This is an indication of the ability of **3a**, and **3b** to generate singlet oxygen is a key factor in the phototransformation of 4-nitrophenol.

Kinetic parameters of the phototransformation of 4-nitrophenol at different initial concentrations using the functionalized fibers (**3a**/PS, **3b**/PS and ZnPc/PS) are given in Table 2.

As shown in Table 2, the observed rate constant (k_{obs}) in all three cases, decreased with an increase in concentration of 4-nitrophenol as expected, with k_{obs} values of **3a**/PS being comparatively slightly higher than those of **3b**/PS and ZnPc/PS. Thus the **3a**/PS fiber shows better photocatalytic behavior toward photocatalytic oxidation of 4-nitrophenol than **3b**/PS and ZnPc/PS and the order is consistent with their ability to generate singlet oxygen.

In heterogenous catalysis, the reaction rate at the surface of the catalyst is related to the concentration of the reactant covering the surface according to the Langmuir–Hinshelwood (L–H) kinetic model, Eq. (7) [55]. This model has been successfully used to describe solid–liquid reactions. Hence we employed it for the treatment of data based on our heterogeneous catalytic mimetic systems.

$$\frac{1}{\text{rate}} = \frac{1}{k_a} + \frac{1}{k_a K C_0} \tag{7}$$

where k_a is the apparent reaction rate constant, K is the adsorption coefficient and C_o corresponds to the initial concentration of 4-nitrophenol. Plots of the inverse of initial reaction rate $(\text{rate})^{-1}$ versus the reciprocal of the initial concentration of 4-nitrophenol $(C_0)^{-1}$ were found to be linear with non zero intercepts for both functionalized fibers, Fig. 10. The apparent rate constant k_a was determined to be 8.76×10^{-6} mol L^{-1} min^{-1} for **3a**/PS, 8.48×10^{-6} mol L^{-1} min^{-1} for **3b**/PS and 4.5×10^{-6} mol L^{-1} min^{-1}

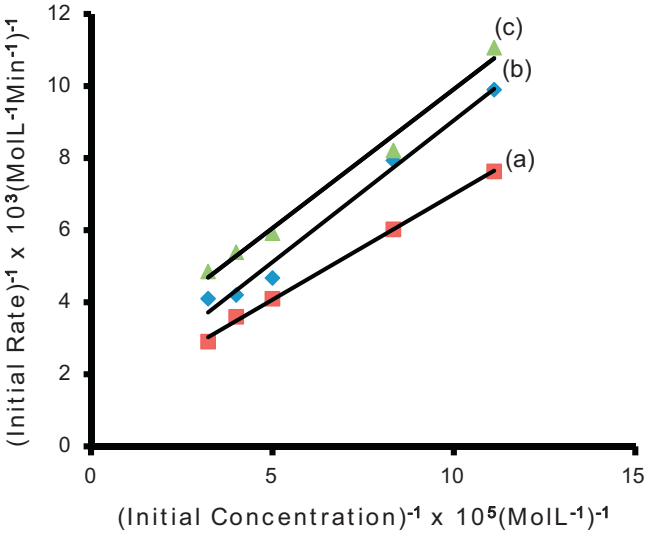

Fig. 10. Plot of the inverse of initial reaction rate $(\text{rate})^{-1}$ versus the reciprocal of the initial concentration of 4-Np for photooxidation using 20 mg (a) **3a**/PS, (b) **3b**/PS and (c) ZnPc/PS functionalized fiber.

Table 2
The rate, rate constant (k_{obs}) and half-life ($t_{1/2}$) of various initial concentrations of 4-nitrophenol.

4-NP concentration ($\times 10^{-4}$ mol L^{-1})	Complex	k_{obs} ($\times 10^{-2}$ min^{-1})	Initial rate ($\times 10^{-6}$ mol L^{-1} min^{-1})	Half-life/min
0.9	**3a**/PS	1.46	1.31	47.5
	3b/PS	1.12	1.01	61.8
	ZnPc/PS	1.00	0.90	69.3
1.2	**3a**/PS	1.38	1.66	50.2
	3b/PS	1.07	1.26	64.8
	ZnPc/PS	1.02	1.22	68.0
2.0	**3a**/PS	1.22	2.44	56.8
	3b/PS	1.05	2.14	66.0
	ZnPc/PS	0.85	1.69	81.5
2.5	**3a**/PS	1.11	2.78	61.9
	3b/PS	0.95	2.38	72.8
	ZnPc/PS	0.74	1.86	93.7

for ZnPc/PS, indicating slightly faster reaction kinetics for the degradation of 4-nitrophenol with **3a**/PS fiber than with both **3b**/PS and ZnPc/fibers. This is a reflection of the slightly higher singlet oxygen quantum yields of the former. The absorption coefficients *K*, were found to be 1.5×10^3 mol^{-1}, 2×10^3 mol^{-1} and 5.8×10^3 mol^{-1} for **3a**/PS, **3b**/PS and ZnPc/PS fibers respectively. This suggests that adsorption was slightly less favored in the case of **3a**/PS compared to desorption while the converse is true for **3b**/PS and ZnPc/PS fibers. The half-lives are within one and half hours of photo-irradiation for fibers suggesting that the functionalized fibers are promising as fabrics that could be applied for real applications.

3.2.5. Gas chromatographic analysis

The reaction products were identified using chromatography. This was done by spiking sample solutions with standard solutions of the products. As shown in Fig. 11, the photo-degradation products consist of 4-nitrocatechol, benzoquinone and hydroquinone. Mass spectrometry (MS) was further used to confirm the products. The following molecular ions corresponding to the products were identified; [M+2H$^+$] = 112 amu for hydroquinone, [M+H$^+$] = 109 amu for benzoquinone and [M+2H$^+$] = 112 amu for 4-nitrocatechol.

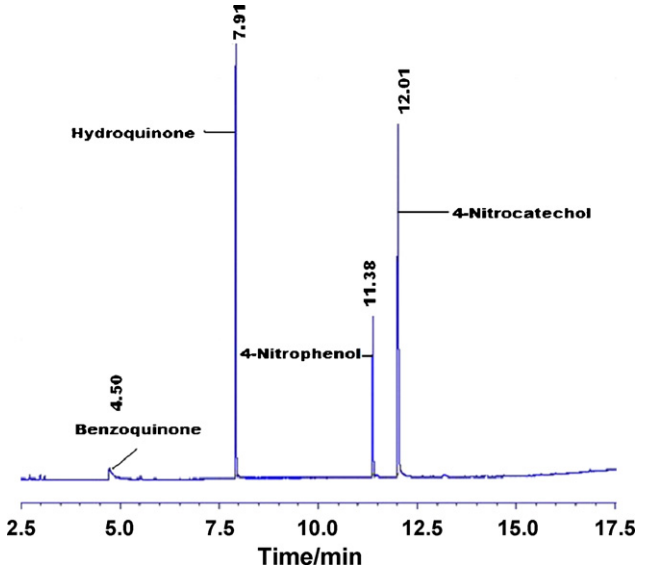

Fig. 11. Gas chromatographic traces of photolysis products of 4-nitrophenol using PS/**3a** fiber as sensitizer for 12 h.

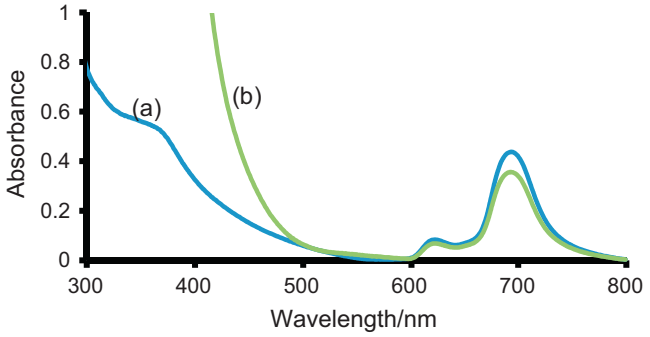

Fig. 12. UV–vis spectra of 10 mg of **3b**/PS functionalized fiber (a) not used in catalysis and (b) used in catalysis (time: 12 h), each dissolved in 4 ml of THF.

3.3. Fate of the phthalocyanines during photocatalysis

The photostability of imbedded sensitizer is an important factor for the application of such fabric materials for photocatalysis. Its decomposition will lead to the termination of the photocatalytic process. Therefore the photostability of phthalocyanines within the fiber matrices were assessed by observing the Q-band absorption of an equivalent amount (10 mg) of the fibers before and after catalysis, both dissolved in equal volume of THF (4 mL), Fig. 12 for **3b**/PS fiber. As indicated, the decrease in the absorption band after the photolysis suggests that the phthalocyanine photo-degrades slightly upon continuous irradiation for 12 h. This could account for the decrease in the reaction rates when the functionalized fibers were used for repetitive conversion of the 4-nitrophrnol. Nonetheless, the fiber could be re-used for at least three cycles for degradation of 4-nitrophenol. FT-IR analysis of the fibers before and after irradiation showed no apparent structural changes in the components. Also scanning electron microscopic (SEM) images of the fibers after use indicate the fiber that average diameters remained virtually the same. However the strands of fibers became more closely compressed after use than before. Thus there was reduced porosity in the fiber mats and could also account for the reduced degradation rate of 4-nitrophenol during re-use of the fibers.

4. Conclusion

In this work, two phthalocyanine complexes of lutetium peripherally substituted with phenoxy (compound **3a**) and 2-pyridiloxy (compound **3b**) groups were synthesized and characterized using conventional spectroscopic methods. They were found to be photoactive with triplet quantum yields of 0.71 and 0.68 for **3a** and **3b** respectively in DMF. The corresponding triplet state lifetimes were 2.60 ± 0.01 μs and 2.64 ± 0.01 μs for **3a** and **3b**. Singlet

oxygen quantum yields also in DMF were found to be 0.68 and 0.62 for **3a** and **3b** respectively. The singlet oxygen generating ability was maintained in the fiber for both phthalocyanines and these polymeric fiber materials incorporating phthalocyanines further found to be promising materials for the photo-conversion of 4-nitrophenol.

Acknowledgments

This work was supported by the Department of Science and Technology (DST) and National Research Foundation (NRF) of South Africa through DST/NRF South African Research Chairs Initiative for Professor of Medicinal Chemistry and Nanotechnology and Rhodes University.

References

[1] S.D. Doyce, M.R. Hoffman, P.A. Hong, L.M. Moberly, Environ. Sci. Technol. 17 (1983) 602–611.
[2] D. Gu, Q. Chen, X. Tang, F. Gan, S. Shen, K. Liu, H. Xu, Opt. Commun. 121 (1995) 125–129.
[3] L. Ma, Y. Zhang, P. Yuan, Opt. Express 18 (2010) 17666–17971.
[4] L. Kaestner, M. Cesson, K. Kassab, T. Christensen, P.D. Edminson, M.J. Cook, T. Chambrier, G. Jori, Photochem. Photobiol. Sci. 2 (2003) 660–667.
[5] A.C. Tedesco, J.C.G. Rotta, C.N. Lunardi, Curr. Org. Chem. 7 (2003) 187–196.
[6] M. Durmus, T. Nyokong, Photochem. Photobiol. Sci. 6 (2007) 659–668.
[7] A.G. Gürek, Ö. Bekaroğlu, J. Chem. Soc., Dalton Trans. (1994) 1419–1423.
[8] A. Beck, K.M. Mangold, M. Hanack, Chem. Ber. 124 (1991) 2315–2321.
[9] P. Tau, T. Nyokong, J. Mol. Catal. A: Chem. 273 (2007) 149–155.
[10] M.D. Maree, T. Nyokong, K. Suhling, D. Philips, J. Porphyrins Phthalocyanines 6 (2002) 373–376.
[11] M. Hu, Y. Xu, J. Zhao, Langmuir 20 (2004) 6302–6307.
[12] N. Kobayashi, in: C.C. Leznoff, A.B.P. Lever (Eds.), Phathalocyanines—Properties and Applications, vol. 2, VCH Publishers Inc., New York, 1993, p. 97.
[13] K. Lang, J. Mosinger, D.M. Wagnerová, Coord. Chem. Rev. 248 (2004) 321–350.
[14] L. Alagna, A. Capobianchi, M.P. Casaletto, G. Mattogna, A.M. Paoletti, G. Pennesi, G. Rossi, J. Mater. Chem. 11 (2001) 1928–1935.
[15] W. Chidawanyika, A. Ogunsipe, T. Nyokong, New J. Chem. 31 (2007) 377–384.
[16] S. Moeno, T. Nyokong, J. Photochem. Photobiol. A: Chem. 203 (2009) 204–210.
[17] R. Zugle, C. Litwinski, T. Nyokong, Polyhedron 30 (2011) 1612–1619.
[18] J.G. Young, W. Onyebuagu, J. Org. Chem. 55 (1990) 2155–2159.
[19] N.B. McKeown, J. Painter, J. Mater. Chem. 4 (1994) 1153–1156.
[20] I. Scalise, E.N. Durantini, Bioorg. Med. Chem. 13 (2005) 3037–3045.
[21] J.R. Lakowicz, Principles of Fluorescence Spectroscopy, 2nd ed., Kluwer Academic Plenium Publishers, New York, 1999.
[22] P. Kubát, J. Mosinger, J. Photochem. Photobiol. A 96 (1996) 93–97.
[23] J. Kossanyi, D. Chachraoui, Int. J. Photoenergy 2 (2000) 9–15.
[24] S. Fery-Forgues, D. Lavabre, J. Chem. Educ. 76 (1999) 1260–1264.
[25] T. Shen, Z.-I. Yuan, H.-J. Xu, Dyes Pigments 11 (1989) 77–80.
[26] X.-F. Zhang, H.-J. Xu, J. Chem. Soc., Faraday Trans. 89 (1993) 3347–3351.
[27] T. Nyokong, Coord. Chem. Rev. 251 (2007) 1707–1722.
[28] T. Nyokong, E. Antunes, in: K.M. Kadish, K.M. Smith, R. Guilard (Eds.), The Handbook of Porphyrin Science, vol. 7, Academic Press/World Scientific, New York/Singapore, 2010, pp. 247–349 (Chapter 34).
[29] A. Ogunsipe, D. Maree, T. Nyokong, Mol. Struct. 650 (2003) 131–140.
[30] A. Ogunsipe, T. Nyokong, J. Photochem. Photobiol. A 173 (2005) 211–220.
[31] C.S. Foote, in: H.H. Wasserman, R.W. Murray (Eds.), Singlet Oxygen, Academic Press, New York/San Francisco/London, 1979, pp. 139–171.
[32] S. Tang, C. Shao, Y. Liu, S. Li, R. Mu, J. Phys. Chem. Solids 68 (2007) 2337–2340.
[33] M.J. Stillman, T. Nyokong, in: C.C. Leznoff, A.B.P. Lever (Eds.), Phthalocyanines: Properties and Applications, vol. 1, VCH, New York, NY, 1989 (Chapter 3).
[34] T. Nyokong, H. Isago, J. Porphyrins Phthalocyanines 8 (2004) 1083–1090.
[35] A. Ogunsipe, J.-Y. Chen, T. Nyokong, New J. Chem. 28 (2004) 822–827.
[36] H.J. Harman, J. Porphyrins Phthalocyanines 6 (2002) 73–77.
[37] J. Mosinger, K. Lang, P. Kubàt, J. Sýkora, M. Hof, L. PlÍštil, B. Mosinger Jr., J. Fluoresc. 19 (2009) 705–713.
[38] D.W. Mayo, F.A. Miller, R.W. Hannah, Course Notes on the Interpretation of Infrared and Raman Spectra, John Wily and Sons, Inc., New Jersey, 2004 (Chapter 5).
[39] V. Duarte, D. Gasparutto, L.F. Yamaguchi, J.L. Ravanat, G.R. Martinez, M.H.G. Medeiros, P.D. Mascio, J. Cadet, J. Am. Chem. Soc. 122 (2000) 12622–12628.
[40] G. Porcal, S.G. Bertolotti, C.M. Previtali, M.V. Encinas, Phys. Chem. Chem. Phys. 5 (2003) 4123–4128.
[41] M.O. Liu, C.-H. Tai, A.T. Hu, T.-H. Wei, J. Organomet. Chem. 689 (2004) 2138–2143.
[42] L.A. Tomachynski, I.N. Tretyakova, V. Ya Chernii, S.V. Volkov, M. Kowalska, J. Legendziewicz, Y.S. Greasymchuk, S. Radzki, Inorg. Chim. Acta 361 (2008) 2569–2581.
[43] J.A. Lacey, D. Phillips, Photochem. Photobiol. Sci. 1 (2002) 378–383.
[44] T. Ngai, G. Zhang, X. Li, D.K.P. Ng, C. Wu, Langmuir 17 (2001) 1381–1383.
[45] I. Seotsanyana-Mokhosi, N. Kuznetsova, T. Nyokong, J. Photochem. Photobiol. A: Chem. 140 (2001) 215–222.
[46] V. Purohit, A.K. Basu, Chem. Res. Toxicol. 13 (2000) 673–692.
[47] I.J. Alinnor, M.A. Nwachukwu, J. Environ. Chem. Ecotoxicol. 3 (2011) 32–36.
[48] N.D. Zakaria, N.A. Yusof, J. Haron, A.H. Abdullah, Int. J. Mol. Sci. 10 (2009) 354–365.
[49] X. Shen, L. Zhu, G. Liu, H. Yu, H. Tang, Environ. Sci. Technol. 42 (2008) 1687–1692.
[50] F.R. Zaggot, N.A. Ghalwa, J. Environ. Manage. 86 (2008) 291–296.
[51] R.P.S. Suri, J. Liu, D.W. Hand, J.C. Crittenden, D.L. Perram, M.E. Mullins, Water Environ. Res. 65 (1993) 665–673.
[52] E. Silva, M.M. Pereira, H.D. Burrows, M.E. Azenha, M. Sarakha, M. Bolte, Photochem. Photobiol. Sci. 3 (2004) 200–204.
[53] M.M. Fickling, A. Fischer, B.R. Mann, J. Packer, J. Vaughan, J. Am. Chem. Soc. 81 (1959) 42264230.
[54] R. Gerdes, D. Wohrle, W. Spiller, G. Schneider, G.G. Schnurpfeil, J. Schulz-Ekloff, Photochem. Photobiol. A 111 (1997) 65–74.
[55] A. Al-Ekabi, N. Serpone, J. Phys. Chem. 92 (1988) 5726–5731.